

Post-yield behaviour of low density polyethylenes: 2. Plastic fracture

P. J. Mills* and J. N. Hay

Chemistry Department, The University, Birmingham B15 2TT, UK

(Received 25 April 1984; revised 6 November 1984)

Diamond-shaped cavities have been observed to grow in a stable fashion through oriented low density polyethylenes, linear and high pressure, and account for the ultimate fracture characteristic of these polymers. Their growth has been examined by the application of fine grids on the specimen surface, and (adjacent) elements of material at the diamond tip deform in simple shear in turn, as the maximum shear is attained. Simple shear tests on drawn material confirm that the angle between the linear faces of the diamond cavities is determined by the onset of strain softening followed by strain hardening. The characteristics of these determine the extent of yielding in each element.

(Keywords: low density polyethylene; fracture characteristics; diamond tip; shear; yield)

INTRODUCTION

Recent studies on a range of polymers¹⁻⁵, which neck in tension, have confirmed the generality that post-yield fracture is associated with the growth of diamond-shaped cavities. These are initiated from surface defects, such as crazes or scratches, which tear during strain hardening of the drawn material and produce rhomboidal prism cavities with four equal straight sides at characteristic angles. The two diagonals lie parallel and perpendicular to the draw direction. These have been labelled 'diamonds', and the general fracture mechanism that of 'diamond fracture'.

The well-defined geometry of the diamonds is produced early in their growth and is maintained during growth up to the last stages of fracture. The angle between the straight edges appears to be related to the natural draw ratio and is a material characteristic. Diamond fractures have been observed in high density polyethylene¹, polycarbonate², PVC³, PET⁴ and plasticized cellulose acetate⁵.

The present study on low density polyethylenes, for which a range of branch types, degree of crystallinity and melt index was available, was undertaken to determine the role of branching and morphology on these ultimate properties. In comparing linear and long chain branched PE's, a melt index of about 1.0 and density of 0.92 g cm⁻³ was arbitrarily chosen.

EXPERIMENTAL

Dowex and Sclair resins were compared with a high pressure polymerized PE from BX Ltd. Manufacturer characteristics are listed in *Table 1a*. Each polymer contained 10-20 branches per 10³C atoms, the Dowex material with hexyl branches, the Sclair ethyl branches and the BX Ltd. polymer a range of branches, see *Table 1b*.

Samples were obtained as moulding pellets from which

1 mm thick sheets (20 cm × 20 cm) were prepared by moulding at 550 K for 5 min, under a pressure of 4 MNm⁻². These sheets were quenched directly into ice/water. Densities were measured in a density gradient column of formamide and n-propanol.

Melt flow index was measured according to BS 2781, using a Davenport extrusion plastimeter. G.p.c. measurements of molecular weight were made on a Waters Associates Ltd., 150°C, high temperature gel permeation chromatograph, using o-dichlorobenzene as solvent at 413 K (0.5 w/v concentration). 3 Styragel columns with pore size 10³, 10⁴ and 10⁵ Å were used and their exclusion limits determined using monodisperse polystyrene samples (Polymer Laboratories Ltd.).

Tensile measurements and fracture behaviour were made on a Minimat microscope extensometer, Polymer Laboratories Ltd., which has been described previously^{2,3}. Simple shear measurements were made on an Instron Test Machine, floor model TT-BM, using the plane shear rig built to the basic design of Coker and Filon⁶, but with modifications described elsewhere². Tan ϕ as defined in *Figure 5* was used to measure shear strain.

Tensile tests were carried out with the Instron Test Machine, floor model TT-BM at 296 K and 50% constant humidity, and using dumb-bell specimens cut to BS 2782.

Naturally drawn material was produced using enlarged dumb-bell specimens but using the same ratio of sample dimensions as above. This drawn material was further cut into the standard dumb-bell, at various angles, θ , to the draw attention.

RESULTS

Diamond fracture

Figure 1 exhibits the variation in elongation to fracture with melt index for the different PE's. Although within a given series of PE's there is a decrease in elongation with decreasing molecular weight there was no correlation between the three resin sources, the ldpes being able to

* Present address: Department of Material Science and Engineering, Cornell University, Bard Hall, Ithaca, New York 14853, USA.

Table 1a Polyethylene characteristics

Type	Source	Serial no.	Grade no.	Density (g cm ⁻³)	Melt index	M _w × 10 ³	G.p.c. Mol. Wt.	
							M _n × 10 ³	D
LLDPE	Dow	D1	2045	0.920	1.15	113.4	17.7	6.4
LLDPE	Sclair	S1	11B	0.922	0.70	107.0	20.1	5.3
LDPE	BXL	BX2	DFG4262	0.922	0.84	73.6	23.8	3.2

Table 1b Nature of branches*

Sample	Type	Branches/1000 by ¹³ C n.m.r.	C atoms i.r.
D1	hexyl	13.8	14.1
S1	ethyl	14.4	13.7
BX2 [†]	— [†]	12.6	19.1

By ¹³C n.m.r. ethyl 1.1; butyl 7.0; amyl 1.7; hexyl 2.8

* We are indebted to University of Warwick and SERC for the ¹³C n.m.r. analysis of these polymers

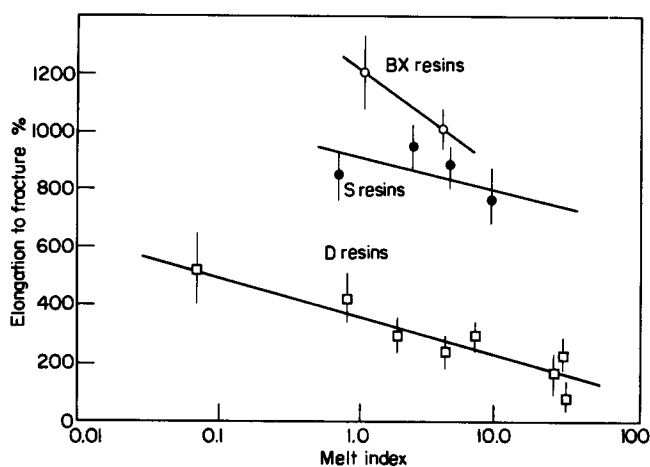


Figure 1 Variation of elongation to fracture with melt index

extend some 10 × original length. We have shown previously⁷ that the elongation to fracture is closely related with strain hardening characteristics of the resins.

Fracture occurred by growth of diamonds, see Figure 2, initiated from surface or edge defects, and some of the variations reflected differences in sensitivity of the rate of growth of the diamonds to the remotely applied load. The PE samples, however, were unique in that they showed a marked insensitivity to the nature and type of defects on the surface. On drawing the specimens uniaxially sharp razor notches rapidly distorted and blunted to a less sharp notch with the same angle as the diamond. The elongation to fracture was not determined by defect concentrations in the specimen since deliberately introduced defects did not grow or develop until strain hardening of the deformed material had occurred in the tensile test as defined previously⁷. As the remotely applied load increased, the diamond grew at an increasing rate. The increasing rate of growth and the inability to apply a constant load precluded the kinetic analysis previously applied² to PC. Under these conditions, the elongation to fracture of these LDPE's was governed by the growth driven by the cross-head speed of the tensometer and not by initiation of defects.

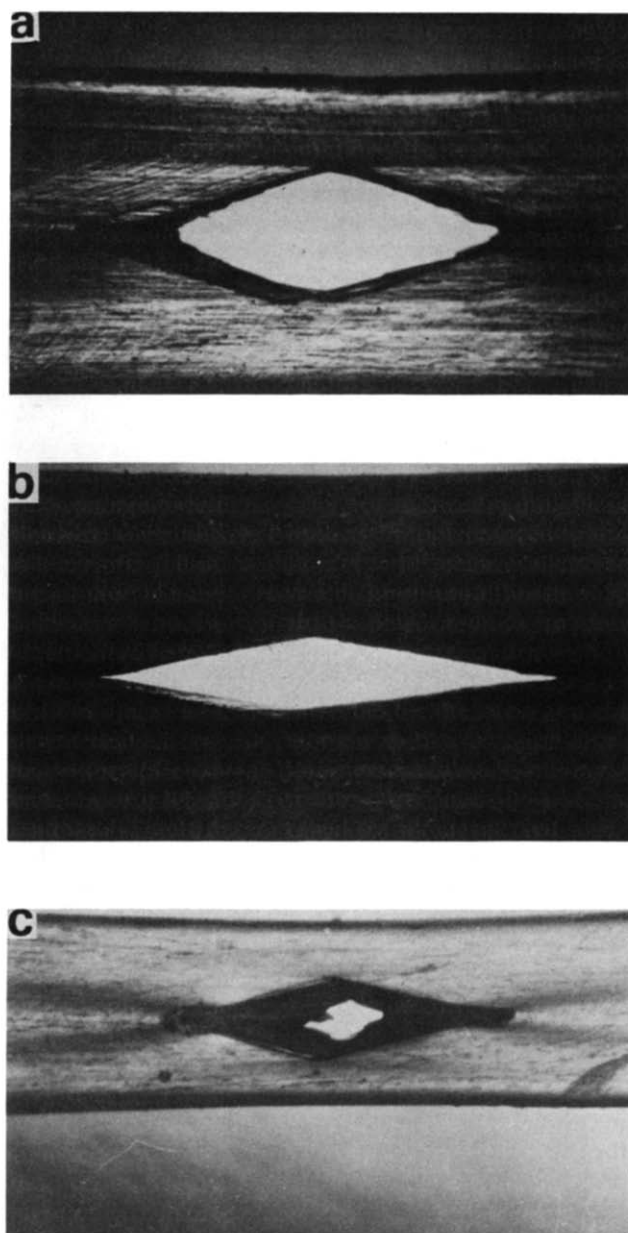


Figure 2 Variation in the shape of the diamond; (a) BX2, (b) S1 and (c) D1

All the diamonds grew from surface defects which opened out into an obtuse angle rhomboid with growth of the diamond occurring from this angle and perpendicular to the draw direction. The geometry of the diamonds, once established, remained constant, for most of its growth and the angles were characteristic of each material. They appeared to increase with the natural draw ratio.

Figure 2 shows the variation in diamond shape obser-

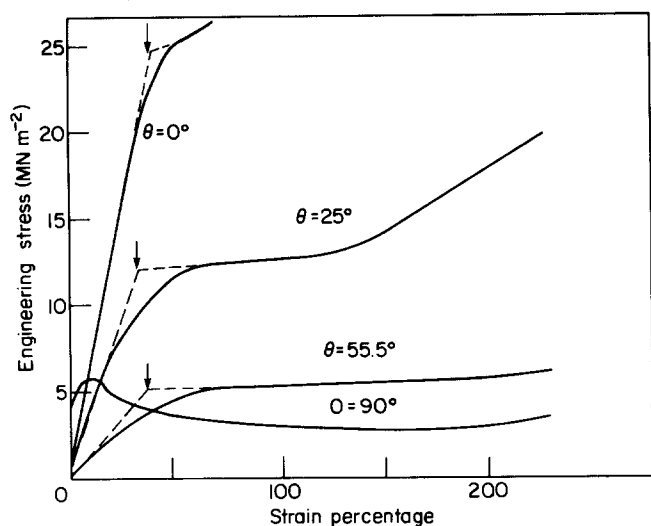


Figure 3 Variation in the stress-strain curves with orientation, to the draw direction θ , strain rate 0.125 min^{-1}

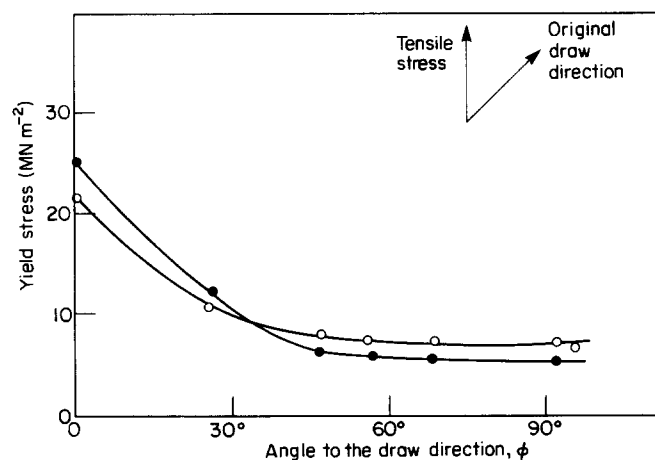


Figure 4 Angular variation of the tensile yield stress, angle to the draw direction θ : (●) BX2, (○) S1; strain rate 0.125 min^{-1}

ved with the various PE samples studied. These diamonds were photographed immediately prior to final failure.

As outlined previously², the strain fields around the diamonds can be analysed by means of the metal squares evaporated onto the surface through a fine mesh. The initial square grids deform to rectangles on necking, and further on strain hardening, but the characteristic deformation of these around the growing tips (obtuse angles of the diamonds) showed that the diamonds grew in simple shear parallel to the draw direction. The greatest shear strain appeared along the edges of the diamonds. This shear was predominantly plastic, as the general shape of the grids was maintained on unloading. As has also been observed previously², and can readily be seen in Figure 2, there was less elongation at the two other diamond tips, due to flow perpendicular to the draw direction. Edge diamonds do not show this, presumably due to presence of the free surface and deformation was almost exclusively in simple shear and lateral extension.

Diamond growth was associated with the anisotropic properties of drawn material and the mechanical properties of naturally drawn PE's were compared to determine the source of variation in fracture characteristics.

Mechanical properties of drawn material

The PE samples were drawn and the test specimens cut at various angles to the draw direction. Figure 3 exhibits the angular variation of the engineering stress-strain behaviour in tension. Only at $\theta = 90^\circ$ did the material neck and geometrically strain soften, followed by a progressive development of the neck through the specimen. At all other angles, no strain softening was observed, indeed the samples strain hardened at various strains after periods of uniform drawing. Extrapolation of the initial elastic region in which stress increased with strain and interpolation of the region of uniform drawing was used to define yield stress, as indicated by the arrows in Figure 3. The yield stress decreased progressively, and was symmetrically about minimum at $\theta = 90^\circ$, see Figure 4. A similar trend was observed with all LDPE's, with only minor variations between them, and in general agreement with Keller and Rider's⁸ measurement on HDPE.

Different behaviour was observed in simple shear tests. The behaviour was more complex. The sample orientation angle, θ , was measured clockwise (the tensile specimen viewed from the front) from the original draw to shear direction. The angular variation can be seen in Figures 5 and 6. The distinct types of shear-strain behaviour was observed, with θ between 0° and 90° and 90° and 180° . In all the tests the deformations were homogeneous and true stress-strain curves were measured up to quite high strains, $\tan \phi$. From $\theta = 0^\circ$ to 60° , the observed yield stress increased to a maximum, and thereafter decreased to a minimum at 120° , followed by a slight increase to 180° . Little variations were observed in yield stress above 90° . Up to about 60° , the yield stress increased by yielding was followed by a slow development of strain hardening. Above $\theta = 70^\circ$, yielding decreased but was followed by marked strain hardening, the extent of both decreasing with increasing angle up to 180° . All the PE samples exhibited these trends with maxima and minima in yield stresses at the same θ values. Variations in yield stresses occurred between the various grades of PE, but these were not particularly large.

DISCUSSION

The mechanical tests can readily be understood in terms of the Bauschinger effect, which predicts that material will have reduced yield stress when a compressive stress

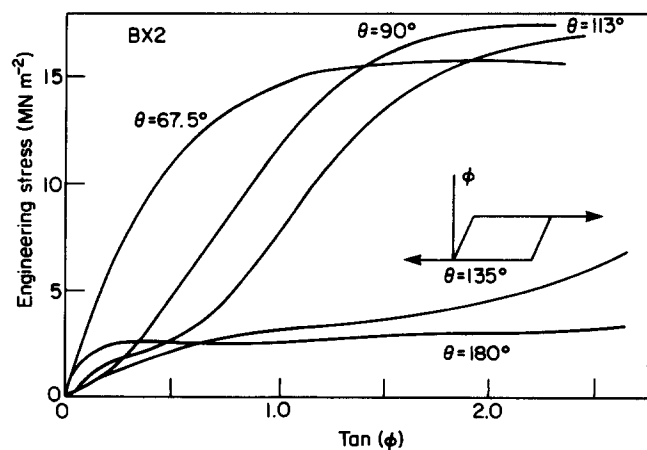


Figure 5 Angular variation of simple shear strain curves, shear strain $\tan \phi$, angle to the draw direction θ

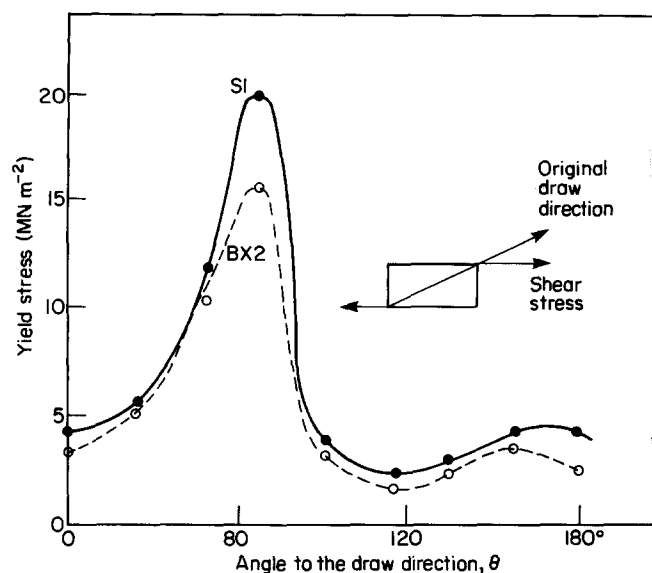


Figure 6 Angular variation of simple shear yield stress, angle to the draw direction θ : strain rate 0.01 min^{-1}

component acts along the drawn direction, i.e. plastic deformation has occurred in the perpendicular direction. Brown *et al.*⁹ have shown that drawn PET, and Walker *et al.*³ drawn PVC, have marked Bauschinger effects in simple shear. Accordingly for the present study, when $\theta=0^\circ$ and 90° , there is no net tensile or compressive stress along the direction of orientation, at zero strain, and similar yield points are obtained. In tensile experiments, the Bauschinger effect is not seen since there is always a tensile component along draw direction.

However, the post-yield behaviour in simple shear at 0° and 90° are markedly different. At $\theta=90^\circ$, the specimen strain hardens on yielding, due to rotation of drawn chains towards the tensile axis. At $\theta=0^\circ$, the angle between initial draw direction and principal stress axis does not change and the specimen uniformly draws.

From the above, it is obvious that the shear yield of drawn material is greatly reduced and either strain softening followed by strain hardening or uniform drawing of the specimen occurs when a compressive component acts along the aligned chains. The most favoured mode of deformation around a defect will be that of shear in the draw direction. As the defect grows, shearing occurs around the defect and the elements extend until strain-hardening occurs. Then it is more favourable for adjacent elements to deform rather than this element to strain harden further. This is analogous to development of a neck in a tensile specimen. Each element shears to a maximum extent, and the diamond faces are constrained to an angle ϕ determined by this strain hardening process.

From the $\theta=0^\circ$ or 180° simple shear curve the extent of deformation which occurs after yielding can be obtained. Elements which deform strain soften and then strain harden. The extent of deformation which occurs before

strain hardening exceeds the yield stress determines the diamond shape. From *Figure 5*, this corresponds to about 2.0 for BX2, corresponding to a minimum diamond angle of 150° . The observed value of 140° is in good agreement with this estimate, since no allowance can be made for different elastic strain fields and material constraints in two types of experiments. Differences observed between the linear low density PE and LDPE, i.e. 150° , 160° and 140° , are then related to the different strain hardening characteristics of these materials in simple shear. By comparison, strain hardening in tensile tests on drawn samples has been measured⁷ in these LDPE and analysed in terms of elasticity theory by the Rivelin-Mooney equation:

$$\text{i.e. } \sigma_T = G(\lambda^2 - 1/\lambda)$$

where G is a modulus related to entanglement molecular weight, σ_T the tensile stress and λ the strain.

Sample no.	G_2 (MN m ⁻²)	Diamond angle	$2 \tan^{-1} \phi^*$
S1	2.14	160°	155
D1	1.92	150°	145
BX2	1.54	140°	130

* Predicted from shear-strain experiments

For the three PE samples studied, the observed angle of the diamond increased progressively with the strain hardening modulus, G . This was the reverse of what was expected, and implies an inverse dependence of shear and tensile strain hardening.

CONCLUSIONS

The characteristic shape of the diamond cavities is determined by simple shear characteristics of the drawn material such that the faces of the diamond remain linear and at a fixed angle. Shear experiments on drawn material confirm this mechanism. Differences in the strain hardening characteristics of PE determine observed variations in diamond angles, and the very large angle between diamond faces at the growth tip, i.e. $140\text{--}160^\circ$, is associated with slow rate of strain hardening observed in the drawn material in simple shear.

REFERENCES

- Walker, N., Haward, R. N. and Hay, J. N. *Polymer* 1979, **20**, 1056
- Walker, N., Haward, R. N. and Hay, J. N. *J. Mater. Sci.* 1981, **16**, 817
- Walker, N., Haward, R. N. and Hay, J. N. *J. Mater. Sci.* 1979, **14**, 1085
- Aref-Azar, A. *Ph.D. Thesis*, University of Birmingham, 1981
- Zurimendi, J. A., private communication
- Coker, E. G. and Filon, L. N. G. 'A Treatise on Photoelasticity', Cambridge University Press, London, 1970
- Mills, P. J., Haward, R. N. and Hay, J. N. *J. Mater. Sci.* 1985, **20**, 501
- Keller, A. and Rider, J. G. *J. Mater. Sci.* 1966, **1**, 389
- Brown, N., Duckett, R. A. and Ward, I. M. *Phil. Mag.* 1968, **18**, 483